

Assessing the impacts of VSC converter configurations on performance and testing of up to 640 kV extruded cable systems

Tanumay KARMOKAR, Marc JEROENSE, Amirhossein ABBASI; NKT HV Cables AB, (Sweden)
tanumay.karmokar@nkt.com, marc.jeroense@nkt.com, amirhossein.abbasi@nkt.com

ABSTRACT

This paper intends to provide an outlook towards considering different-than-standard impulse waveforms for assessing the impacts of over voltages appearing on DC cables in HVDC transmission links due to the interaction between cables and VSC converter stations. An overview is provided on configurations of VSC converter stations while highlighting the characteristics of cross-linked polyethylene (XLPE) DC cable insulation for voltages up to 640 kV. An approach towards designing special experimental technique is presented which is supported by detailed circuit modelling of high voltage test setup taking into account the electrical properties of DC cable. The results are presented and discussed.

KEYWORDS

Non-standard impulse waveforms, over voltages, XLPE DC cable, 640 kV, VSC converters.

INTRODUCTION

HVDC transmission links were first used commercially about half a century ago. Since then an increasing number of such transmission systems have been commissioned around the world and are in successful operation till today. Long distance efficient transmission of bulk power without the need for charging the capacitance of transmission line with alternating voltage makes HVDC a lucrative option for power transfer. Subsequent to the development of thyristor valves, compact Insulated Gate Bipolar Transistor (IGBT) based converters about two decades ago were further developed which gave the necessary impetus to have extruded cable systems as the preferred choice of power transfer mode for HVDC systems since there is no change of voltage polarity when the power direction is changed.

Performance of DC cables in service is strongly governed by its conductivity, which dictates the electrical field distribution under DC voltage. Joule heating of conductor acts as a heat source that generates a temperature gradient over the insulation. Additional heating might come from leakage current through insulation. The latter heat source plays a role in demonstrating the robustness of XLPE DC cable insulation system as it is indicative of the dielectric loss. The effect is cyclic since with rise of loss and temperature the insulation conductivity would further increase. Such series of events has the potential to eventually lead to a thermal runaway if the conductivity crosses its upper threshold limit.

$$P = E^2 \sigma \quad [1]$$

Equation (1) gives the relation between the dielectric current loss density (P) in W/m³, electric field (E) in V/m and conductivity (σ) in S/m. With increasing demand of higher voltages and operating temperature of DC cables, it is of utmost importance to have a cable insulation with a

significantly lower conductivity to avoid the occurrence of a thermal breakdown.

This paper validates the aforementioned strength of DC cable insulation by indicating the characteristic performance of XLPE cable during a prequalification test of 640 kV system. The possible configurations of Voltage Source Converter (VSC) stations are highlighted and a typical overvoltage profile is discussed that could possibly be encountered by a DC cable system in service. Furthermore, results from a non-standard very long impulse test have been presented that shall provide a food for thought to simulate the overvoltage stresses within a standard high voltage test laboratory with standard testing equipment. Thus, reinforcing the robust performance of DC XLPE cable system.

PREQUALIFICATION TESTING OF 640 KV DC XLPE CABLE SYSTEM

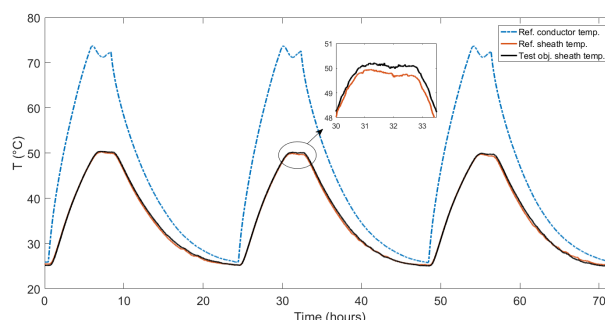


Fig. 1: Prequalification testing of 640 kV DC XLPE cable system

Figure 1 illustrates reference conductor and sheath temperatures, along with the test object sheath temperature measured during a prequalification test of 640 kV DC XLPE cable system. To ensure that the thermal requirements of the test were successfully met, a reference cable with zero voltage was implemented with an aim to accurately measure the conductor temperature for a particular current in the conductor. The same current as that of the reference cable was applied to the test object with a voltage of 928 kV (1.45 x U₀).

There is, in principle, a total overlap of sheath temperature of the test object and that of the reference cable with hardly any scope to distinguish between the two parameters. This demonstrably proves that a 640 kV DC XLPE cable system, which has its conductor temperature maintained at at least 70°C, has an extremely low heat contribution from leakage current under prequalification and type test conditions. This negligible temperature rise guarantees that neither thermal breakdown nor instability due to leakage current loss can occur during test or service conditions. DC XLPE

cable systems are very well suited for ultra-high voltage applications, they are a low loss, recyclable system. Experience of cross-linked polyethylene as a material concept goes back to the 1960's whereas the DC XLPE already has 2 decades of commercial experience.

VSC STATIONS

Economically viable long distance (e.g., above 400 km) [1] power transmission needs have ushered the implementation of HVDC point-to-point schemes that have been widely accepted as national and international interconnectors. VSC stations employ IGBT, which can be turned on or off freely. This is in contrast to conventional thyristor controlled Line Commutated Converter (LCC) stations where the thyristor could only be turned off by zero current forced by an external circuit. Therefore, VSC can generate a voltage waveform that is sinusoidal in nature. This is done independent of the AC system by implementing Pulse-Width Modulation (PWM) technique. VSC converters, additionally, have the capability to simultaneously control the active and reactive power, it has fast dynamic response with black start capability and does not exhibit commutation failures. Due to the absence of need to reverse voltage polarity for controlling power flow, VSC stations can therefore be applied for building multi-terminal schemes.

Fig 2 shows a simplified circuit diagram of one phase of a two-level VSC. The valves comprise of several series connected IGBTs.

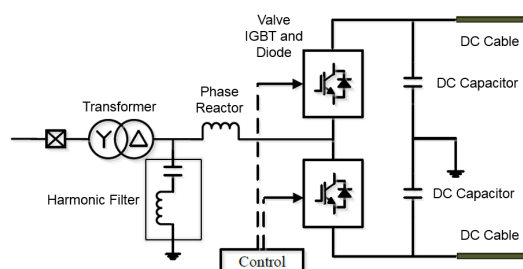


Fig. 2: Simplified circuit diagram of one phase of a two-level Voltage Source Converter (VSC) [1]

VSC Configuration Schemes

Generally, a HVDC transmission link comprises of a point-to-point interconnector system with a rectifier, an inverter and transmission lines in the form of either cables and/or overhead lines. There are mainly five kinds of point-to-point HVDC transmission schemes [1]: monopolar earth return system, monopolar metallic return system (Fig. 3), bipolar system with neutral point of one terminal earthing, bipolar system with neutral point of both terminals earthing (earth return) and bipolar system with metallic return earthed at one end (Fig. 4). For demonstration purposes only metallic return schemes in both types of configurations have been shown in the following figures:

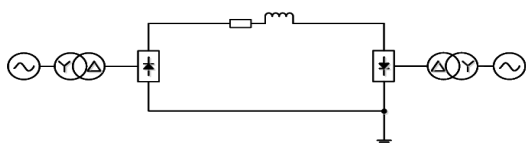


Fig. 3: Monopolar metallic return system of point-to-point HVDC transmission system [1]

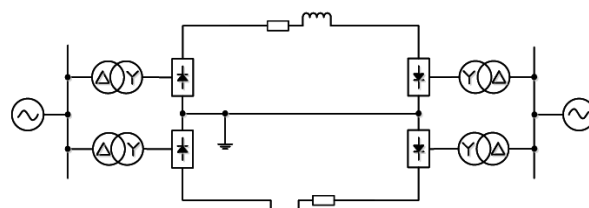


Fig. 4: Bipolar HVDC transmission system with earthing of metallic return [1]

A bipolar metallic return HVDC transmission link could also comprise of a double metallic return line with two transmission lines. This shall effectively constitute a total of four lines including two metallic returns. Such a configuration of HVDC system secures continuous transfer of power in case an outage occurs on single pole converter. Furthermore, the scientific communities have developed great interest in considering deeply the possibilities of realising a multi-terminal HVDC network mainly due to its operational benefits. Possibilities expand from radial networks to more complex topologies of meshed HVDC grids [1].

IMPACT OF HVDC SYSTEM FAULTS ON DC CABLES

A pole-to-ground fault in bipolar HVDC system causes a discharge of the capacitor to ground. An unbalanced DC link then develops between the positive and negative pole voltages. As the voltage of the faulted line begins to fall, high currents flow from the capacitors and AC grid. Comparatively, in a symmetric monopole configuration the reference to ground is not available on the delta side of the transformer. In an event of a single pole-to-ground fault on the DC side, the IGBT in VSC stations would be blocked during first few hundreds of microseconds. However, current conduction would continue through the freewheeling diodes. The converter then continues its operation as a six-pulse rectifier unit until the AC side circuit breakers open which, however, happens only after about few hundreds of milliseconds, approximately 150 ms [4]. Surge arrester operation is critical in such a situation. It functions before the AC side circuit breakers act to limit the over voltage up to about $1.8 U_0$ (less than twice the DC voltage). After the circuit breakers have operated the surge arrester discharges the healthy pole to approximately $1.6 U_0$. This comparatively higher voltage then continues to remain on the cable for about 400 ms [4] and then it is discharged by switching the grounding of DC pole. The time before the emergency grounding switches operate depends on the system configuration on a case-by-case basis wherein the time might vary from few seconds to few minutes.

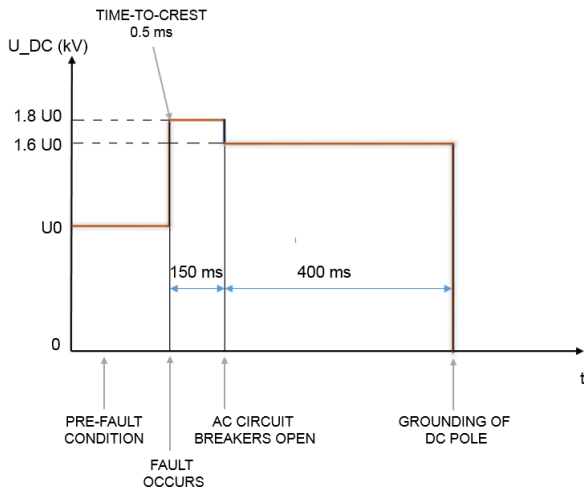


Fig. 5: Representation of a transient over voltage characteristics on a healthy pole in case of a pole-to-earth fault [4]

Surges from AC side

Switching surges generated on the AC side are inductively transferred to the valve side via the transformer. Since voltage of the valve group consists of phase-to-phase components, the zero sequence is not included in the converter voltage [6]. A superimposed surge is transferred to the valve side depending on transformer turns ratio and winding configuration of the transformer i.e., star-star and star-delta configuration. The total peak voltage (U_{pk}), thus, could be expressed by the following formula [6] across a two series-connected valve group.

$$U_{pk} = n \left[U_m \sqrt{2} \sqrt{2 + \sqrt{3}} + U_{ps} + 2 \frac{U_{ps}}{\sqrt{3}} \right] \quad [2]$$

In equation 2, n is the transformer turns ratio (star-star), U_m is the maximum permissible steady state operating phase voltage and U_{ps} is the peak value of the superimposed switching surge. Lightning surges too can be transferred to the DC side from the AC system via the transformer electrostatically as well as electromagnetically. Generally, the electrostatic transfer would only be applicable for transient waves with a steep wave front which gets transferred via the stray capacitance [6].

The DC cable system can now be considered to be stressed with transient over voltages having a profile, which cannot be completely correlated to the standard switching impulses [3]: Time-to-crest: $250 \mu s \pm 20\%$ and Time-to-half value: $2500 \mu s \pm 60\%$.

DESIGN OF VERY LONG SWITCHING IMPULSE TEST CIRCUIT

Impulse Voltage Generator

An equivalent RC circuit representation explains conveniently the generation of impulse voltages (Fig. 6). When an impulse capacitor (C_i) is charged via a charging resistor (R_c) up to a high enough DC breakdown voltage V_0 , which would then lie within the trigger range of the sphere gap, an impulse voltage V_i is generated by the connected network components. Subsequently, the load capacitor C_l is charged via the front resistor R_s which

forms the front of the impulse voltage. At the same time, the impulse capacitor C_i is discharged via the tail resistor R_p and forms the tail of the impulse voltage. The superposition of both processes delivers a peak impulse voltage.

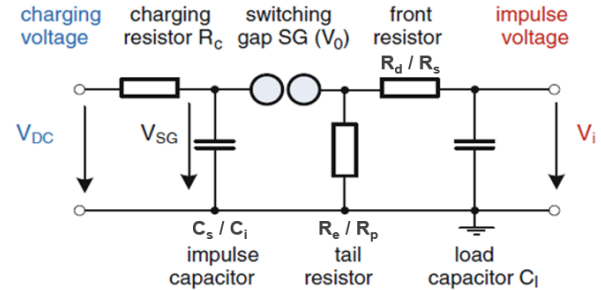


Fig. 6: Basic equivalent circuit for impulse voltage generation for one stage [7]

While being charged all capacitors are connected in parallel and the switching gap is insulating. The charging time is given by ladder network of impulse capacitor, charging resistor, number of stages and the charging unit. The discharging of impulse capacitors occur in series following an ignition of switching gap of first stage and then experiencing a voltage cascading effect on subsequent gaps in higher stages. The effective resistance due to the switching gap is negligible in comparison to the charging resistor (R_c) of the impulse capacitor. Hence, R_c does not have any influence on discharging. The energy dissipated on R_s and R_p is different.

Simulation Model

Approach

Long switching impulse testing is challenged by investigating the influence of electrical parameters of DC extruded cable on the wave shape of the generated test waveform. The eligibility of the wave shape has been determined by its characteristic times i.e., time-to-crest and time-to-half values, which has been decided as $7000 \mu s / 25000 \mu s$ based on the best possible testing attempt within a standard high voltage testing laboratory and the discussions surrounding the representation of over voltage as seen in Fig. 5. The HV test circuit has been dimensioned as per the requirements of generating long switching impulses by adapting the front (damping) resistors and tail (discharging) resistors of the impulse generator. However, since the dimensioning of impulse generator was restricted by available (few kΩ) resistors, the per-stage capacitance of impulse generator was increased (μF). This, along with an external resistor enabled the test setup to suit the requirements of long switching impulse. Thus, the standard HV test setup was adapted by changing the resistor and capacitor component values of the impulse generator to suit the special test requirements.

Modelling Parameters

The simulation activity was initiated by collecting the test equipment data from manufacturer's datasheet and estimating the values of stray capacitive and inductive elements [7]. Fig. 6 was implemented for simulation

purposes, however, with the inclusion of stray elements. The simulation attempt was primarily started with an intention to build a lumped parameter model and verify the resistances and capacitances of impulse generator for its feasibility to generate the desired very long impulses.

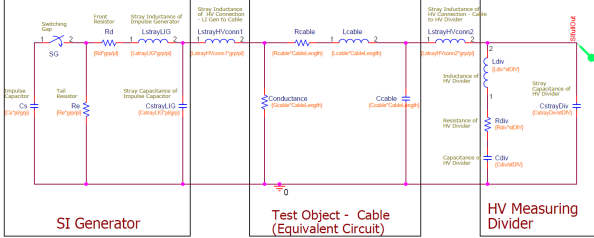


Fig. 7: PSpice simulation model built with all circuit and stray elements as lumped parameters

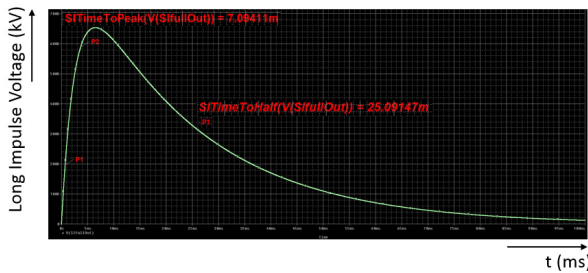


Fig. 8: Lumped parameter PSpice model result characterised by 7.094 µs / 25.0915 µs with a peak voltage of 580 kV

The outcome of lumped parameter modelling indicated that such a long impulse waveform is possible to be generated using standard impulse generator within a standard testing facility.

High Voltage Testing

With the knowledge and confidence gained from the preliminary simulation attempt, a prototype high voltage test setup [5] was designed with a simple capacitive divider of 10 nF as the test object load.

The prototype testing revealed that higher time characteristics of long impulse waveform lowers the efficiency of impulse generator to as low as approximately 45 %; the achieved peak voltage was 44.85 kV for 20 kV applied to each impulse generator stage with a total of 5 stages in operation. Simulation had shown the efficiency to be approximately 54 % with a peak impulse voltage as 53.68 kV for the same impulse generator configuration. The simulated characteristic times were also greater than the achieved test results. Time-to-crest was simulated to be approximately 30 % higher while the time-to-half value was about 11 % greater.

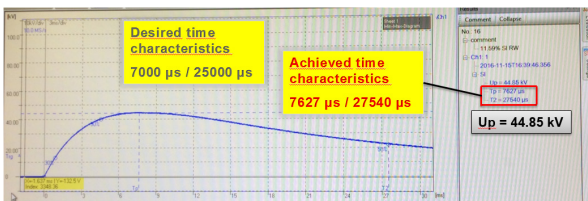
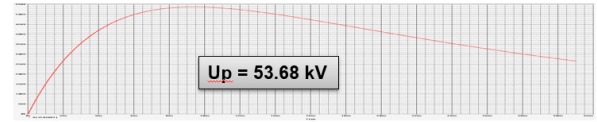


Fig. 9: HV test field result in comparison to the simulated PSpice outcome



Evaluate	Measurement	Value
<input checked="" type="checkbox"/>	SITimeToPeak(V(IFA2out))	10.54284m
<input checked="" type="checkbox"/>	SITimeToHalf(V(IFA2out))	30.75504m

Fig. 10: PSpice simulation results outcome

Improving Simulation Model

The mismatch between the simulated and tested results indicate that better network modelling would be necessary for measurement voltage dividers with improved understanding of its frequency response. Additionally, the measuring dividers are required to be separately calibrated for measuring such non-standard impulse waveform. For this particular testing attempt, R-C universal type voltage divider was used with an estimated error up to 1 %.

An attempt has been further made to apply the Thevenin's theorem to impulse generator. This principle holds valid in this case because an impulse generator can essentially be considered as a one-port (i.e., two-terminal) network of impedances (characteristic resistances and impulse capacitances) that can be connected to an external circuit. The external circuit, in principle, comprises of the load, which is the test object together with measurement voltage divider. Thus, an impulse generator could be considered as a black box that is connected to the outside network through its ports. PSpice tool gives a provision to measure the equivalent impedance by placing the measuring probe for example, at the terminals of "SI Generator" in Fig. 7. The voltage rating of the impulse generator could be considered as the necessary open circuit potential taking into account 100 % efficiency level for an unloaded impulse generator. The cable is modelled using a simple ladder equivalent network where the electrical parameters are calculated using standard formulae [8].

Let U_{inp} be the input voltage to impulse generator while the U_{ot} be the output from the impulse generator. Thus, the gain of the impulse generator could be given by its ratio. Now if the dominant inductance (L) and capacitance (C) of the cable are considered individually then viewing towards the impulse generator from the test object (L, C) the Thevenin's equivalent with the cable inductance (and resistance) in focus can be respectively written as,

$$\frac{U_{ot}}{U_{inp}} = \frac{R + j\omega L}{(R + Z_{th}) + j\omega L} \quad [3]$$

Z_{th} is the Thevenin's equivalent impedance of the impulse generator. Similarly, Thevenin's equivalent with the cable capacitance in focus can be respectively written as,

$$\frac{U_{ot}}{U_{inp}} = \frac{-j/\omega C}{(Z_{th}) - j/\omega C} \quad [4]$$

In the above equations [3] and [4] the left side of the equation denotes the gain, which in principle is the efficiency of the impulse generator. The efficiency of impulse generator is approximately 95 % for standard lightning, 80 % for standard switching [7] and as indicated

above based on prototype testing the efficiency falls down to 45 % for long impulses. Substitution of respective values would give relation between the inductance and capacitance of an impulse generator as a function of frequency (ω).

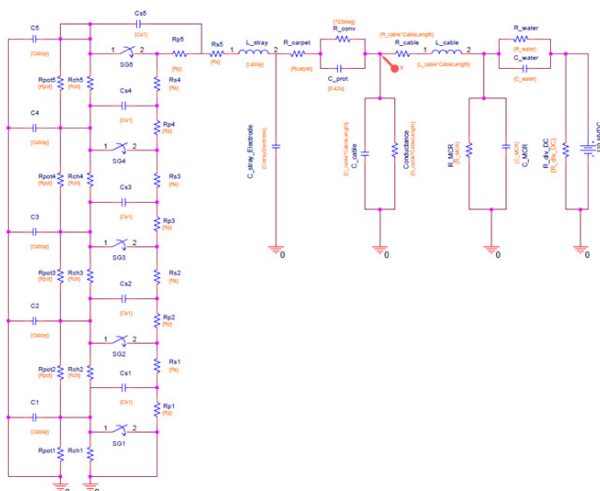


Fig. 11: Detailed simulation model of long impulse / DC superimposed implementing distributed parameter modelling of impulse generator

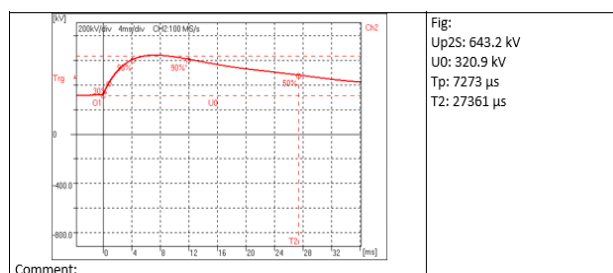


Fig. 12: Test laboratory output waveform for same positive polarity long impulse based on detailed PSpice simulation

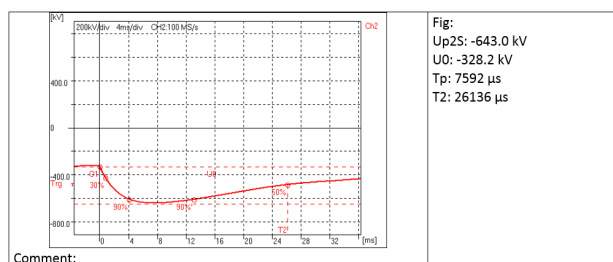


Fig. 13: Test laboratory output waveform for same negative polarity long impulse based on detailed PSpice simulation

Fig. 12 and Fig. 13 indicate the results of performing the long impulse test on a 320 kV DC XLPE cable system as a test object. The accessories consisted of terminations and two prefabricated joints. The conductor temperature was maintained at at least 70°C during the test while maintaining minimum temperature gradient across the XLPE insulation

DISCUSSIONS AND CONCLUSION

In the current paper an outlook is provided on the VSC

station configurations while highlighting the temporary over voltage and other impacts encountered by extruded DC cable system due to abnormal operations in a VSC HVDC station. We have undertaken an attempt to experimentally generate a temporary over voltage wave shape as they have been raised in several recent discussions of pole-to-ground faults in VSC symmetric monopole HVDC system configuration. The design of experimental setup was executed in a standard high voltage testing laboratory by retrofitting conventional test components to suit our needs to generate a much longer than standard impulse wave shape. Apart from demonstrating our attempt to devise a conceptual approach towards tackling over voltage issues, it has also been readily shown that a laboratory oriented experimental setup cannot, in general, reflect all features of an over voltage profile as they are being currently predicted by several authors. On one hand features like permanence to peak i.e., a plateau-like appearance at the peak of the over voltage wave and longer characteristic time of over voltages discussed can hardly be met with standard testing infrastructure and might not necessarily be relevant. On the other hand rise times and a substantially long tail time as compared to current test standards can indeed be reproduced for testing purposes as it has been demonstrated in this paper.

Despite the question of generation of simulated wave shape, there needs to be a discussion on actual impact of the temporary over voltages on insulation system, i.e. the cable insulation and its accessories. From breakdown threshold and probability of flashover perspective the standard switching impulse seems to be sufficient to test for the peak level of 1.8 U₀, as here often higher peak voltages are required. On the other hand readers are encouraged to ponder over the energy deposited locally in the cable system and resistive heating which cannot be dissipated on relevant timescales. Even in [2] for pure DC test voltages of required 1.85 U₀ could be sufficient to clear the requirement from the perspective of over voltages. However, the authors do not intend to conduct such discussions at this point. Instead it is suggested that insulation coordination discussions to be taken up in order to clarify the practical relevance of such transient wave shapes.

Acknowledgment

We are grateful to Dr. rer. nat Markus Saltzer, Convenor of Cigré JWG B4/B1/C4.73 for being available to conduct fruitful discussions and for sharing his valuable insights on the topic.

REFERENCES

- [1] CIGRE JWG A3/B4.34, 2017 "Technical Requirements and Specifications of State-of-the-art HVDC Switching Equipment", Technical Brochure 683
- [2] CIGRE WG B1.34, 2012, "Recommendations for Testing DC Extruded Cable Systems for Power Transmission at a Rated Voltage up to 500 kV", Technical Brochure 496
- [3] IEC Standard 62067, 2011, "Power cables with extruded insulation and their accessories for rated voltages above 150 kV (Um= 170 kV) up to 500 kV

(Um= 550 kV) – Test methods and requirements”

- [4] M. Marzinotto, F. Palone, M. Rebolini, 2017, “Temporary overvoltages in ungrounded neutral HVDC-VSC systems: a question of uncertainties”, Presentation, HVDC international workshop – Venice
- [5] N. Giao Trinh, Daniel Couderc, 1992, “Analysis of Test Circuits for Evaluating HVDC Cables”, IEEE International Symposium on Electrical Insulation, Baltimore, MD USA
- [6] Jos Arrillaga, 1998, HIGH VOLTAGE DIRECT CURRENT TRANSMISSION, The Institution of Electrical Engineers, London, United Kingdom, 229-238
- [7] Wolfgang Hauschild, Eberhard Lemke, 2014, High-Voltage Test and Measuring Techniques, Springer-Verlag Berlin Heidelberg, 285-303
- [8] Juan A. Martinez-Velasco, 2010, Power System Transients Parameter Determination, CRC Press, Taylor & Francis Group, USA, 144-166